Stress Analysis of Functionally Graded Disk with Exponentially Varying Thickness using Iterative Method

[1]SANDEEP KUMAR PAUL
[1]Department of Mathematics, School of Technology, Pandit Deendayal Energy University, Gandhinagar, Gujarat – 382426, INDIA

[2]MANOJ SAHNI
[2]Department of Mathematics, School of Technology, Pandit Deendayal Energy University, Gandhinagar, Gujarat – 382426, INDIA

Abstract: - In this paper, variable thickness disk made up of functionally graded material (FGM) under internal and external pressure is analyzed using a simple iteration technique. Thickness of FGM disk and the material property, namely, Young's modulus are varying exponentially in radial direction. Poisson's ratio is considered invariant for the material. Navier equation is used to formulate the problem in the differential equation form under plane stress condition. Displacement, stresses, and strains are obtained under the influence of material gradation and variable thickness. Three different material combinations are considered for the FGM disk. The mechanical response of disk obtained for different functionally graded material combinations are compared with the homogenous disk, and results are plotted graphically.

Key-Words: - Functionally graded material, Disk, Pressure, Variable thickness, Iterative technique.

Received: April 18, 2021. Revised: October 10, 2021. Accepted: October 23, 2021. Published: November 9, 2021.

1 Introduction

In recent years, functionally graded materials (FGMs) have gained a lot of recognition as an advanced composite material over traditional composites due to their smooth material property gradation over the material dimension. FGMs were first conceptualized in 1980, by Japanese scholars to create a material that can be used to solve the problem of high temperature difference between the outer surface and inner surface of space shuttle. These materials are an inhomogeneous combination of metal-ceramic and are tailored in such a way that the metal matrix reinforced with ceramic provides a smooth transition of material properties from one surface to other. Due to their ability to provide smooth material gradation, FGMs have stress concentration reduction at interface region and high material strength under severe thermomechanical loading conditions. Metal matrix composites with ceramic as reinforcement material are used as structural material in many engineering areas like aerospace, defense, automotive, civil engineering, electronics, etc. In this age of interdisciplinary research, many researchers and engineers from different science, engineering backgrounds are working together in search of new real-life applications of functionally graded materials in their respective fields. The problems raised by mechanical responses of functionally graded disk has received fair attention. Due to the complexity of material gradation, geometric profile, mechanical and thermal loading, researchers are working on obtaining proper analytical solutions to find displacement and stresses in many research articles. To design an engineering component, it is important to choose the best material to achieve the desired performance by the component under thermomechanical load. So, the study of different material combinations made up of composite materials becomes important to get optimal material performance out of it. This is the motivation for considering three different functionally graded materials in this study.

Nejad et al. [1] investigated the stress response of a thick FGM spherical shell with exponential tailoring property under internal and external pressures. Some researchers considered FGM rotating sandwich disk under thermomagnetic loading and compared its thermomechanical response with composite disk [2]. Jalali et al. employed the finite difference method (FDM), for analysis of elastic stress in rotating thick annular disk subjected to clamped-free, clamped-clamped, and free-free boundary conditions [3] whereas Temimi and Ansari [4] have developed a semi-analytical method that can be used to solve non-linear equations of second-order multipoint boundary value problems. The method of simple iteration technique and finite element method are used by several researchers for investigating the stress distribution and displacement for a thick-walled FGM sphere and the obtained

results are found to be in good agreement with these two methods [5]. Lin [6] has used the concept of hypergeometric differential equation to solve the Navier equation for the stresses and studied the influence of mechanical load on the displacement of a thin-walled FGM annular disk under different pressure boundary conditions. Sahni and Mehta [7] studied the effect of thermal and mechanical loading on a functionally graded sandwich cylinder using the finite element method. Mars et al. [8] analysed the static response of a functionally graded shell by applying the finite element method using ABAQUS software. Thermomagnetic elastic response of axisymmetric functionally graded (FG) sphere following power rule for gradation is determined and observed considerable effect of inhomogeneity constant on stresses and displacement [9]. Çallıoğlu et al. [10] have used FORTAN program to derive stresses in closed form for FG rotating disk and obtained results are further compared by a numerical solution using finite element method ANSYS program. The three most common material combinations are considered for the comparative study of stress behavior in the cases of functionally graded hollow cylinders, spheres, and thin disks under the condition of internal and external pressures [11]. A functionally graded rotating disk with hyperbolic and parabolic thickness profiles in power-law form is presented and used in the evaluation of stress distribution under different pressure conditions and compared the obtained result with homogenous disk [12], [13]. This comparison claims that a functionally graded disk performs better than a disk with homogenous thickness. A hollow FG cylinder with asymmetric loading is considered and the effect of non-homogeneity parameter on the tangential and radial stresses is presented using analytical method and received results are further compared by the results obtained by shooting method considering Runge -Kutta fourth-order [14]. Delouei et al. [15] have studied the effect of two-dimensional thermal conduction along the radial and longitudinal directions on the axisymmetric functionally graded cylinder using the Fourier transform method. Analytical solution for elastoplastic stresses of the functionally graded rotating disk is derived by considering Tresca's model for yield criterion [16]. Tutuncu [17] has used the power series method to derive the analytical solution for exponentially graded isotropic functionally grade material subjected to inner and outer pressure. The author has shown the influence of varying volume fractions on stresses and displacement. A rotating annular and solid FGM disks with varying thickness are analysed for stress response using the graded finite element method (GFEM) along the radial and axial directions, where, Young's modulus and other material properties are changing along the radial and axial direction by following power rule [18]. Paul and Sahni ([19], [20], [21]) have investigated two-dimensional mechanical responses for cylindrical and spherical pressure vessels made up of functionally graded materials. Sahni and Sharma ([24], [25]) have investigated creep and elastic plastic stress analysis for functionally graded thin rotating disk. Sharma et. al [26] have used Transition theory to obtain the transitional and elastic-plastic stresses in a thin rotating disk.

In this paper, a thin isotropic axisymmetric FGM disk with variable thickness is considered and the governing differential equations formulated using stress-equilibrium equation, stress-strain, and strain-displacement relations is solved under plane stress conditions. Modulus of elasticity and thickness of disk are defined in exponential form and Poisson's ratio is kept invariant. A semi-analytical iterative method is applied to derive the solution of stresses and displacement in the radial direction. The derived solution for radial stress, tangential stress, and displacement are plotted graphically in the study. For the numerical part, three different functionally graded materials are considered for the disk with ceramic and metal as inner and outer material respectively. The obtained mechanical responses of three FGM disks with different material combinations are then compared with the homogenous disk. This comparison shows that FGM disks perform better than homogenous disks from the perspective of practical use.

2 Formulation of the Problem

In this study, a thin axisymmetric functionally graded disk with an inner radius $'r_1'$ and the outer radius $'r_2'$ is considered under plane stress and steady-state conditions. The Poisson's ratio $'v'$ of the material is assumed to be constant but the modulus of elasticity $'Y(r)'$ and thickness of disk $'h(r)'$ are varying exponentially along the radial direction.

Modulus of elasticity and thickness of disk are following exponential law as

$$Y(r) = Y_c e^{-m(r-r_1)/r_2} \quad (1)$$

$$h(r) = h_c e^{-k(r-r_1)/r_2} \quad (2)$$

where $r_1 \le r \le r_2$ and $'Y_c'$ is constant of Young's modulus, $'h_c'$ is the thickness of the disk at inner radius. Material grading and varying thickness indices are denoted by $'m'$ and $'k'$ respectively and expressed as,

$$m = \frac{r_2}{r_2 - r_1} log\left(\frac{Y(r_1)}{Y(r_2)}\right), k = \frac{r_2}{r_2 - r_1} log\left(\frac{h(r_1)}{h(r_2)}\right)$$

Navier equation for the isotropic functionally graded disk with variable thickness in the absence of body force is expressed as [3],

$$\frac{d}{dr}(rh(r)\sigma_r(r)) - h(r)\sigma_\theta(r) = 0 \quad (3)$$

where $'\sigma_r(r)'$ and $'\sigma_\theta(r)'$ are radial and tangential stresses respectively along the radial direction.

Strain-displacement relation with radial strain $'\varepsilon_r(r)'$, tangential strain $'\varepsilon_\theta(r)'$, and radial displacement $'u(r)'$ can be considered as [22],

$$\varepsilon_r(r) = \frac{du(r)}{dr} \quad \text{and} \quad \varepsilon_\theta(r) = \frac{u(r)}{r} \quad (4)$$

The stress-strain relation that describes Hooke's law under plane stress condition is presented as [11],

$$\sigma_r(r) = \frac{Y(r)}{1-v^2}(v\varepsilon_\theta(r) + \varepsilon_r(r)) \quad (5)$$

$$\sigma_\theta(r) = \frac{Y(r)}{1-v^2}(\varepsilon_\theta(r) + v\varepsilon_r(r)) \quad (6)$$

The pressure boundary condition with internal pressure $'q_1'$ and outer pressure $'q_2'$ is defined as,

$$\sigma_r(r_1) = -q_1 \text{ MPa and } \sigma_r(r_2) = -q_2 \text{ MPa} \quad (7)$$

Solving equations (1)-(6), the equilibrium equation in the displacement form can be written as,

$$\frac{d^2u}{dr^2} + \frac{1}{r}\frac{du}{dr} - \frac{u}{r^2} = \frac{(m+k)}{r_2}\frac{du}{dr} + \frac{v(m+k)}{r_2}\frac{u}{r} \quad (8)$$

2.1 Basics of used iterative technique [5]

A general form of an ordinary differential equation can be considered as:

$$\phi_1(y(x)) = g(x) + \phi_2(y(x)) \quad (9)$$

subjected to the boundary condition $F\left(y, \frac{dy}{dx}\right) = 0$.

where y(x) and g(x) are unknown and known functions respectively. In equation (9), 'ϕ_1' is a linear operator and $'\phi_2'$ is a nonlinear operator as well as a boundary operator. As per the requirement, few terms of linear part can also be added to ϕ_2.

In this technique, the initial solution $y_0(x)$ is considered as a complementary function of the equation (9) and can be obtained by solving equation (10) as,

$$\phi_1(y_0(x)) = 0 \text{ with } F\left(y_0, \frac{dy_0}{dx}\right) = 0 \quad (10)$$

To get improvement in the solution $y_0(x)$, the next iteration $y_1(x)$ can be obtained by solving equation (11) as,

$$\phi_1(y_1(x)) = g(x) + \phi_2(y_0(x) \quad (11)$$

with $F\left(y_1, \frac{dy_1}{dx}\right) = 0$

By repeating this procedure for $n+1$ terms, equation (11) can be written in the iteration form as,

$$\phi_1(y_{n+1}(x)) = g(x) + \phi_2(y_n(x)) \quad (12)$$

with $F\left(y_{n+1}, \frac{dy_{n+1}}{dx}\right) = 0, n = 0,1,2,3..$

where each $y_j(x)(j = 0,1,2,3\ldots)$ represents a separate solution to equation (11), but it is believed that one can obtain the improved value of the solution by considering a greater number of iterations. The next iteration shows a good improvement over the previous iteration.

2.2 Implementation of the iterative technique

By applying iterative technique from equation (12) to equation (8), governing differential equation can be expressed as,

$$\frac{d^2u_{n+1}}{dr^2} + \frac{1}{r}\frac{du_{n+1}}{dr} - \frac{u_{n+1}}{r^2} = \frac{(m+k)}{r_2}\frac{du_n}{dr} + \frac{v(m+k)}{r_2}\frac{u_n}{r}$$

with $F\left(u_{n+1}, \frac{du_{n+1}}{dr}\right) = 0 \quad (13)$

where $\phi_1(u_{n+1}(r)) = \frac{d^2u_{n+1}}{dr^2} + \frac{1}{r}\frac{du_{n+1}}{dr} - \frac{u_{n+1}}{r^2}$ and $\phi_2(u_{n+1}(r)) = \frac{(m+k)}{r_2}\frac{du_n}{dr} + \frac{v(m+k)}{r_2}\frac{u_n}{r}$ are linear and nonlinear parts of equation (13) respectively.

Thus, the Initial solution for equation (13) is

$$\phi_1(u_0) = 0, \text{with} \begin{cases} \frac{Y(r_1)}{1-v^2}\left(\frac{du_0}{dr} + v\frac{u_0}{r}\right)_{r=r_1} = -q_1 \\ \frac{Y(r_2)}{1-v^2}\left(\frac{du_0}{dr} + v\frac{u_0}{r}\right)_{r=r_2} = -q_2 \end{cases} \quad (14)$$

The general solution of the initial problem (14) can be obtained as,

$$u_0(r) = \frac{C_1}{r} + C_2 r \quad (15)$$

By applying boundary condition from equation (14) on equation (15), constants of integration C_1 and C_2 can be evaluated as,

$$C_1 = \left(\frac{q_1}{Y(r_1)} - \frac{q_2}{Y(r_2)}\right)\frac{(1+v)r_1^2r_2^2}{r_2^2 - r_1^2} \quad (16)$$

$$C_2 = \left(\frac{q_1 r_1^2}{Y(r_1)} - \frac{q_2 r_2^2}{Y(r_2)}\right)\left(\frac{1-v}{r_2^2 - r_1^2}\right) \quad (17)$$

The first iteration is $u_1$and can be evaluated by solving the equation (13) for $n = 0$ as,

$$\frac{d^2u_1}{dr^2} + \frac{1}{r}\frac{du_1}{dr} - \frac{u_1}{r^2} = \frac{(m+k)}{r_2}\frac{du_0}{dr} + \frac{v(m+k)}{r_2}\frac{u_0}{r} \quad (18)$$

with $F\left(u_1, \frac{du_1}{dr}\right) = 0$

and has a solution as,

$$u_1 = C_4 r + \frac{C_3}{r} + \frac{(m+k)(1+v)}{3r_2}C_2 r^2 + \frac{(m+k)(1-v)}{r_2}C_1 \quad (19)$$

where integration constants C_3 and C_4 can be find as,

$$C_3 = \left(C\left(1 + \frac{v(m+k)r_1}{(r_1+r_2)}\right) - \frac{(v+2)(m+k)}{3r_2(r_1+r_2)} \times D\right)\frac{(1+v)r_1^2 r_2^2}{r_2^2 - r_1^2} \quad (20)$$

$$C_4 = (1-v)\begin{pmatrix} \frac{-q_1}{Y(r_1)} - D\begin{pmatrix} \frac{(v+2)(m+k)r_1}{3r_2(r_2^2-r_1^2)} \\ + \frac{(v+2)(m+k)}{3r_2(r_1+r_2)}\frac{r_2^2}{r_2^2-r_1^2} \end{pmatrix} \\ -C\begin{pmatrix} \frac{v(m+k)r_1 r_2}{r_2^2-r_1^2} - \\ \left(1 + \frac{v(m+k)r_1}{(r_1+r_2)}\right)\frac{r_2^2}{r_2^2-r_1^2} \end{pmatrix} \end{pmatrix} \quad (21)$$

Applying the same process, the second iteration is obtained as,

$$u_2 = C_6 r + \frac{C_5}{r} + \frac{(m+k)(1+v)}{3r_2}C_4 r^2 + \frac{(m+k)(1-v)}{r_2}C_3 + \frac{(m+k)^2(1-v)(v+2)}{24r_2^2}C_2 r^3 + \frac{(m+k)^2 v(1-v)}{2r_2^2}C_1 r \log r \quad (22)$$

and the constants of integration C_5 and C_6 are calculated as,

$$C_5 = \begin{pmatrix} C + \begin{pmatrix} \frac{-q_1}{Y(r_1)} - D\begin{pmatrix} \frac{(v+2)(m+k)r_1}{3r_2(r_2^2-r_1^2)} + \\ \frac{(v+2)(m+k)}{3(r_1+r_2)}\frac{r_2}{r_2^2-r_1^2} \end{pmatrix} - \\ C\left(\frac{v(m+k)r_1 r_2}{r_2^2-r_1^2} - \left(1 + \frac{v(m+k)r_1}{(r_1+r_2)}\right)\frac{r_2^2}{r_2^2-r_1^2}\right) \end{pmatrix} \\ \times \frac{(v+2)(m+k)(r_2-r_1)(1-v)}{3(v-1)r_2} - \\ \frac{(v+2)(v+3)(m+k)^2(r_2^2-r_1^2)}{24(1+v)r_2^2} D\left(\frac{1-v}{r_2^2-r_1^2}\right) \\ -\frac{v(m+k)^2 \log\left(\frac{r_2}{r_1}\right)}{2r_2^2}\frac{(1+v)r_1^2 r_2^2 C}{r_2^2-r_1^2} + \\ \frac{v(m+k)(r_2-r_1)}{r_1 r_2^2(1+v)} \times \begin{pmatrix} C\left(1 + \frac{v(m+k)r_1}{(r_1+r_2)}\right) \\ -\frac{(v+2)(m+k)}{3r_2(r_1+r_2)} D \end{pmatrix} \\ \frac{(1+v)r_1^2 r_2^2}{r_2^2 - r_1^2} \\ \times \frac{r_1^2 r_2^2}{r_2^2 - r_1^2} \end{pmatrix} \quad (23)$$

$$C_6 = \begin{pmatrix} \frac{-q_1(1-v^2)}{Y(r_1)} - \begin{pmatrix} \frac{(2-v)r_1(m+k)(1-v^2)}{3r_2} \\ \left(\frac{-q_1}{Y(r_1)} - DA - CB\right) \\ + \frac{(3-v)r_1^2(m+k)^2(1-v)(v+2)}{24r_2^2} \\ D\left(\frac{1-v}{r_2^2-r_1^2}\right) + \\ \frac{(m+k)^2 v(1-v^2)r_1^2 r_2^2(1+\log r)}{2r_2^2(r_2^2-r_1^2)} C \end{pmatrix} \\ +v\begin{pmatrix} \frac{(m+k)(1-v)}{r_1 r_2}\begin{pmatrix} C\left(1 + \frac{v(m+k)r_1}{(r_1+r_2)}\right) \\ -\frac{(v+2)(m+k)}{3r_2(r_1+r_2)} D \end{pmatrix} \\ \frac{(1+v)r_1^2 r_2^2}{r_2^2 - r_1^2} + \frac{(m+k)^2 v(1-v)}{2r_2^2} \\ C\frac{(1+v)r_1^2 r_2^2}{r_2^2 - r_1^2}\log r_1 \end{pmatrix} \\ -\frac{(v-1)}{r_1^2}\begin{pmatrix} \begin{pmatrix} C + \left(\frac{-q_1}{Y(r_1)} - DA - CB\right) \times \\ \frac{(v+2)(m+k)(r_2-r_1)(1-v)}{3(v-1)r_2} \\ -\frac{(v+2)(v+3)(m+k)^2}{24(1+v)} \\ \frac{(r_2^2-r_1^2)}{r_2^2} D\left(\frac{1-v}{r_2^2-r_1^2}\right) - \\ \frac{v(m+k)^2 \log\left(\frac{r_2}{r_1}\right)}{2r_2^2} \\ C\frac{(1+v)r_1^2 r_2^2}{r_2^2-r_1^2} + \frac{v(m+k)(r_2-r_1)}{r_1 r_2^2(1+v)} \\ \times \begin{pmatrix} C\left(1 + \frac{v(m+k)r_1}{(r_1+r_2)}\right) \\ -\frac{(v+2)(m+k)}{3r_2(r_1+r_2)} D \end{pmatrix} \\ \frac{(1+v)r_1^2 r_2^2}{r_2^2 - r_1^2} \end{pmatrix} \\ \times \frac{r_1^2 r_2^2}{r_2^2 - r_1^2} \end{pmatrix} \end{pmatrix}$$

$$\times \frac{1}{1+v}$$

We stop here as the remaining iterations contain too long expressions to show. The accuracy of the solution may be increased by considering more number of iterations.

Substituting $u(r) = u_2(r)$ in the equations (4)-(6), radial and tangential strains and stresses are obtained as,

$$\varepsilon_r(r) = \begin{matrix} C_6 - \frac{C_5}{r^2} + \frac{2(m+k)(1+v)}{3r_2} r C_4 + \\ \frac{(m+k)^2(1-v)(v+2)}{8r_2^2} C_2 r^2 \\ \left(+ \frac{(m+k)^2 v(1-v)}{2r_2^2} C_1 (1 + \log r) \right) \end{matrix}$$

$$\varepsilon_\theta(r) = \begin{matrix} C_6 + \frac{C_5}{r^2} + \frac{(m+k)(1+v)}{3r_2} C_4 r + \\ \frac{(m+k)(1-v)}{r r_2} C_3 \\ + \frac{(m+k)^2(1-v)(v+2)}{24r_2^2} C_2 r^2 + \\ \left(\frac{(m+k)^2 v(1-v)}{2r_2^2} C_1 \log r \right) \end{matrix}$$

$$\sigma_r(r) = \frac{Y(r)}{1-v^2} \begin{matrix} (v+1)C_6 + (v-1)\frac{C_5}{r^2} + \frac{(v+2)(m+k)(1+v)}{3r_2} \\ \times C_4 r + \frac{(m+k)v(1-v)}{r r_2} C_3 + \\ \frac{(m+k)^2(v+3)(1-v)(v+2)}{24r_2^2} C_2 r^2 \\ \left(+ ((v+1)\log r + 1) \frac{v(m+k)^2(1-v)}{2r_2^2} C_1 \right) \end{matrix}$$

$$\sigma_\theta(r) = \frac{Y(r)}{1-v^2} \begin{matrix} (1+v)C_6 + (1-v)\frac{C_5}{r^2} + \frac{(1+2v)(m+k)}{3r_2} \\ \times (1+v) C_4 r + \frac{(m+k)(1-v)}{r r_2} C_3 + \\ \frac{(m+k)^2(1+3v)(1-v)(v+2)}{24r_2^2} C_2 r^2 \\ \left(+ ((1+v)\log r + v) \frac{v(1-v)(m+k)^2}{2r_2^2} C_1 \right) \end{matrix}$$

3 Results and Discussion

Consider a thin FGM disk with an inner radius $r_1 = 0.2m$, outer radius $r_2 = 1m$, internal pressure $q_1 = 100$MPa, and external pressure $q_2 = 10$MPa. Three different material combinations of ceramics (inner material) and metals (outer material) are considered for the study, and their material properties are shown in table 1. In this table, Poisson's ratios for ceramic and metal are $'v_c'$and $'v_m'$ respectively, and Poisson's ratio $'v'$ for FGMs are assumed as $v = (v_c + v_m)/2$. Non-FGM (homogenous) disk made up of Silicon Carbide (SiC) is considered with Young's modulus 480 GPa and Poisson's ratio 0.16. Thickness indices $k = -2, -1, 0, 1, 2$ and internal thickness $h(r_1) = 0.01m$ are considered for all FGM and non- FGM disks. In Figure 1 and Figure 2, Young's modulus and thickness profile for assumed FGMs and Non-FGM disks are presented. In Figure 1, one can see that Young's modulus for non-FGM (Silicon Carbide) is highest among rest functionally graded materials and remain constant throughout the radius from inner to outer. But Young's modulus for FGMs are continuously decreasing as radius vary from inner to outer radii. Towards outer radius, one can observe that Young's modulus of FGM-1 is falling more rapidly in compare to FGM-2 and FGM-3, and achieve the lowest value. This means that FGM-1 is less stiff material in comparison to FGM-2 and FGM-3. Figure 2 shows disk with constant thickness at k = 0, concave disk at k = -2, -1 and convex disk at k = 1,2. Internal thickness for all FGMs and non-FGM is assumed as 0.01m at k = -2, -1,0,1,2. But external thickness for the FGM disks vary by using equation (2). External thickness is decreasing as, k moves from -2 to 2.

Table 1. Material Properties [22], [23]

Materials	Grading pair (Inner-Outer)	Young's Modulus (GPa) (Inner-Outer)	Grading Index (m)	Poisson's ratio (v_c-v_m)	Average Poisson's ratio (v)
FGM-1	Silicon Carbide (SiC)-Zinc Alloy (ZA)	480-81.5	2.21647	0.16-0.3262	0.24
FGM-2	Boron Carbide (B_4C)-Nickel Alloy (NA)	460-205	1.01027	0.17-0.310	0.24
FGM-3	Silicon Nitride (Si_3N_4) -Nickel (Ni)	348.43-199.5	0.69702	0.24-0.3	0.27

In Figure 3, Figure 4, Figure 5, Figure 6 and Figure 7, radial displacement is presented for the functionally graded disk made up of different material combinations of ceramics and metals, further compared by non-FGM disk at different thickness indices as k = -2, -1,0,1,2. From these graphs, it is observed that radial displacement has a higher magnitude at the inner radius and the lower magnitude at the outer radius that may happen due to higher internal and lower external pressure. The compressiveness of radial displacement decreases as 'k' varies from -2 to 2 for all materials.

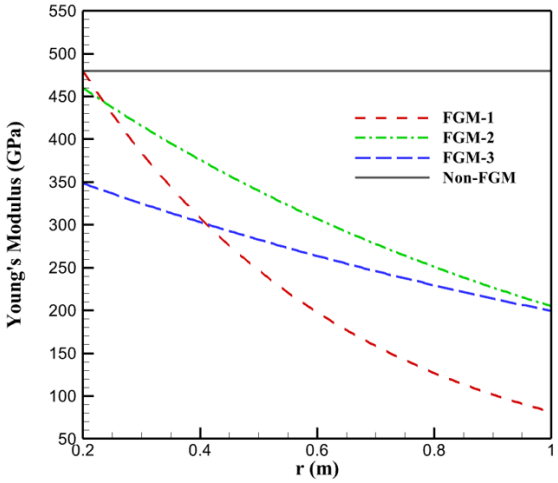

Fig.1 Young's modulus

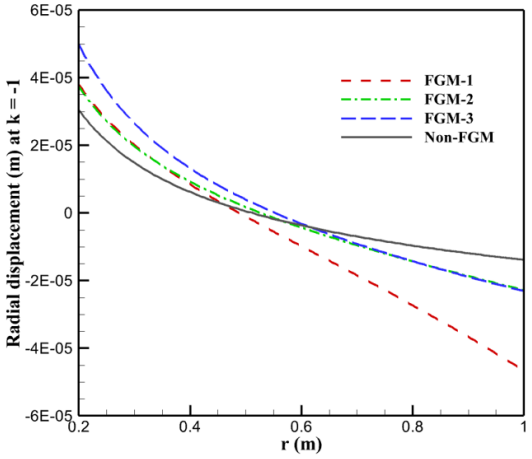

Fig.4 Radial displacement at k = -1

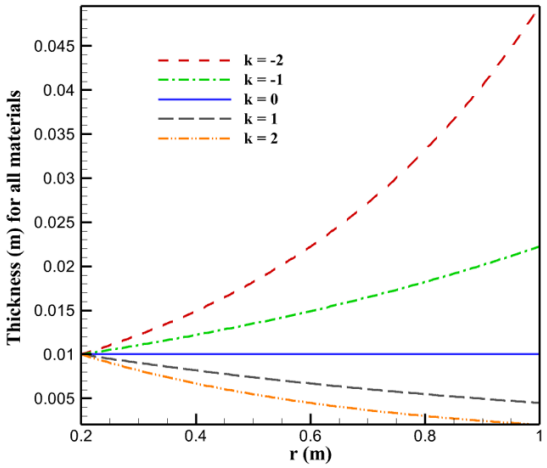

Fig.2 Thickness profile

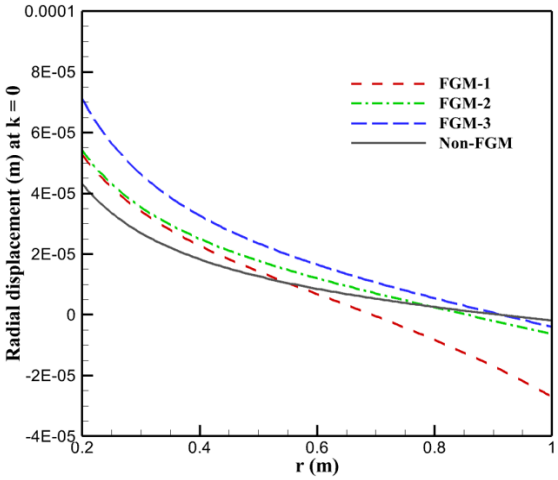

Fig.5 Radial displacement at k = 0

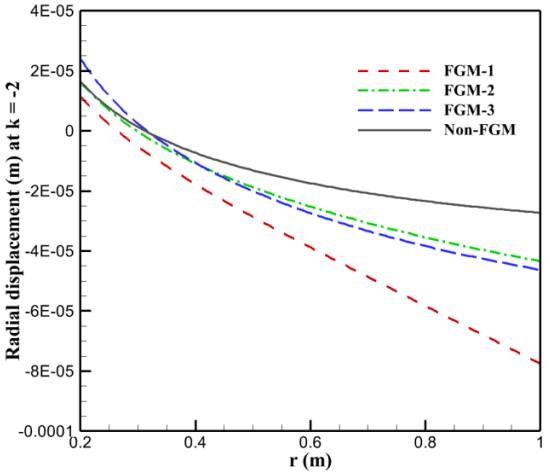

Fig.3 Radial displacement at k = -2

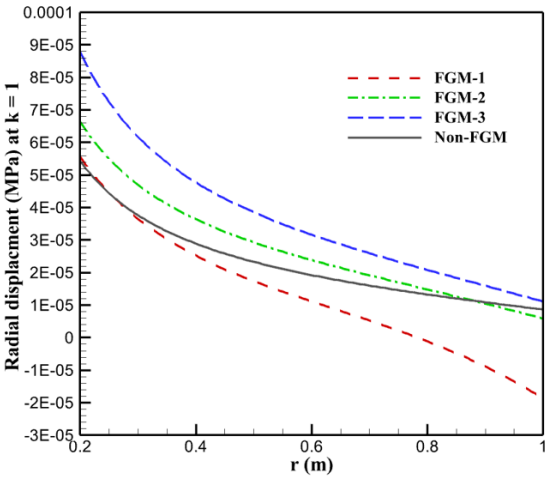

Fig.6 Radial displacement at k = 1

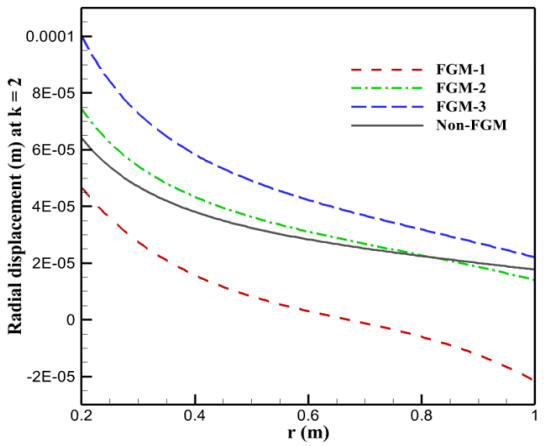

Fig.7 Radial displacement at k = 2

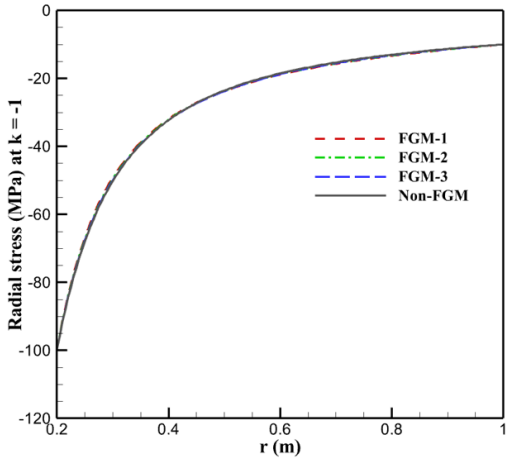

Fig.9 Radial stress at k = -1

Figure 8, Figure 9, Figure 10, Figure 11 and Figure 12 display radial stresses for considered material types for a disk at different values of thickness parameter. By observing these graphs, it is found that the magnitude of radial stress is decreasing as the radius moves from inner to outer under high internal and low external pressure. The nature of radial stress is completely compressive which means each material tries to bear the internal pressure and apply the resistance force in the opposite radial direction. Since the pressure is high at the internal radius so more resistance force is required to sustain the compatibility in the material. In Figure 9, radial stresses for all materials are almost equal at thickness k = -1. Figure 10, Figure 11 and Figure 12 show the lowest magnitude for FGM-1 among the rest of the materials. But in Figure 12, it can be seen that near the internal radius it has the highest magnitude but as it moves towards the outer radius it goes to lower magnitude.

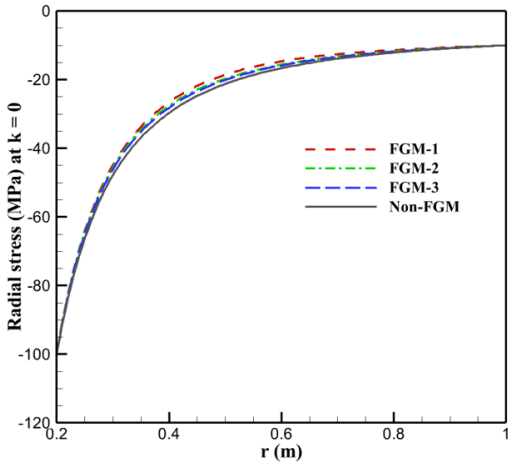

Fig.10 Radial stress at k = 0

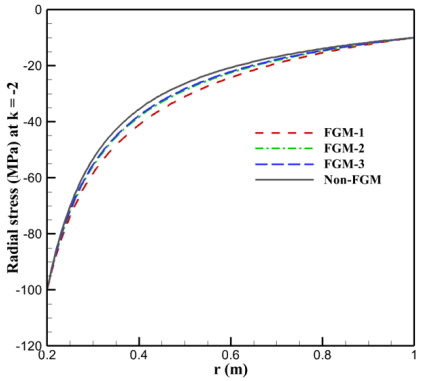

Fig.8 Radial stress at k = -2

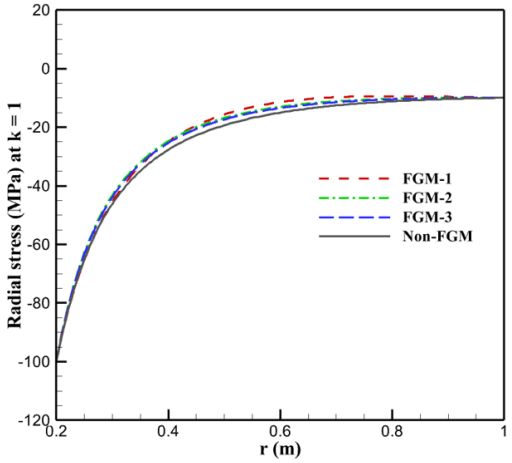

Fig.11 Radial stress at k = 1

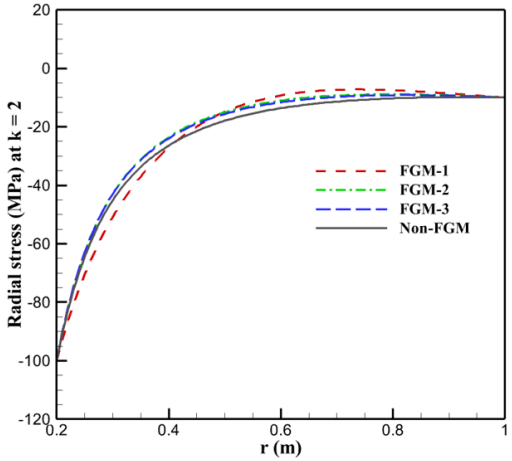

Fig.12 Radial stress at k = 2

An engineer may choose FGM-1 among the rest of the materials to make an engineering component as it reduces stress concentration under the mechanical load especially for convex type of disks.

In Figure 14, Figure 15, Figure 16 and Figure 17, it is observed that tangential stresses are decreasing as thickness moves from the inner to the outer radius. But in Figure 13, one can note that at k = -2, stress values are initially decreasing near the inner radius but towards the outer radius stress values are increasing. Also, the intersection of stress curves for all materials shows an equal stress magnitude near 0.65 radius. By observing Figure 13, Figure 14, Figure 15, Figure 16 and Figure 17, one can find that tangential stress for FGM-1 has the lowest value in comparison to the rest of the materials for all k = -2, -1, 0, 1, 2. But non-FGM disk has high magnitude stress values in the major part of the curve in comparison to other materials. That means non-FGM is not suitable material for designing thin disks under high-pressure load.

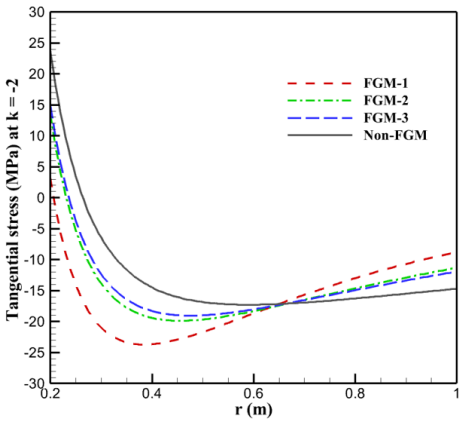

Fig.13 Tangential stress at k = -2

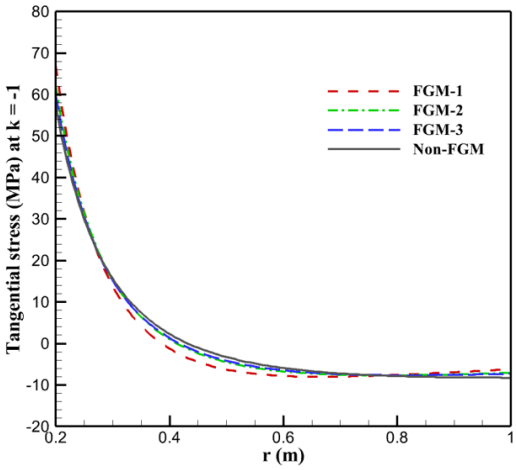

Fig.14 Tangential stress at k = -1

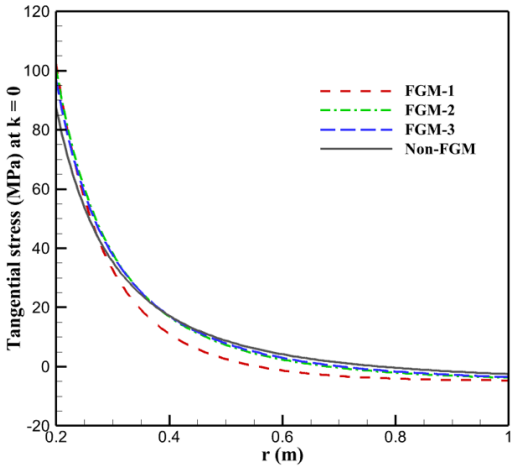

Fig.15 Tangential stress at k = 0

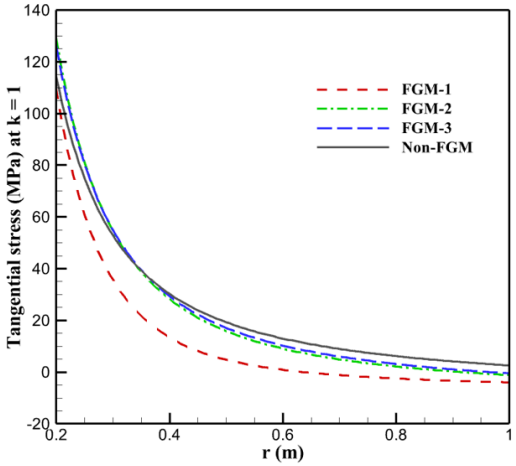

Fig.16 Tangential stress at k = 1

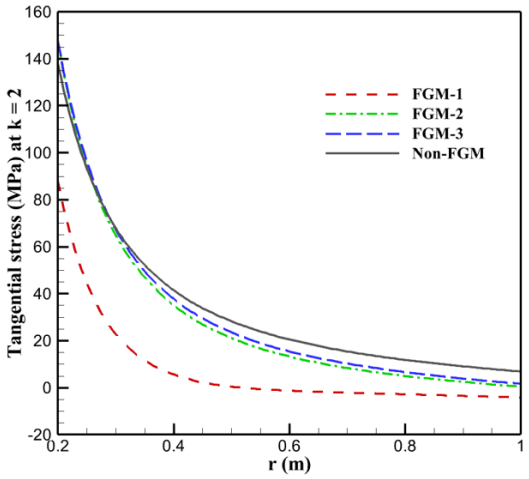

Fig.17 Tangential stress at k = 2

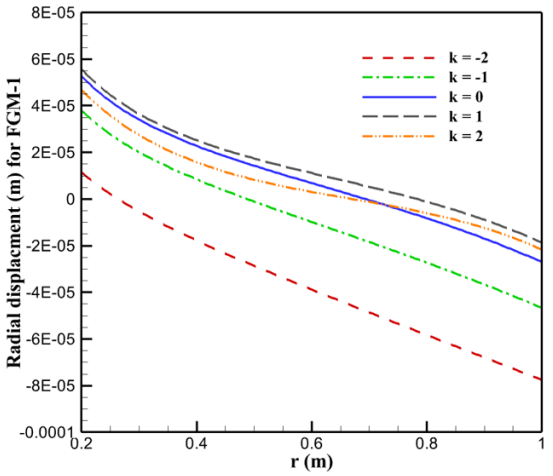

Fig.18 Radial displacement for FGM-1 disk

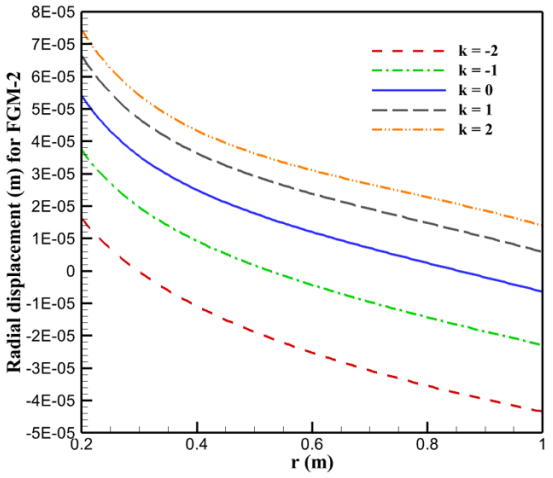

Fig.19 Radial displacement for FGM-2 disk

Figure 18, Figure 19, Figure 20 and Figure 21 show the radial displacement for FGM-1, FGM-2, FGM-3 and non-FGM respectively for concave, convex and uniform disk. By observing these figures, it is seen that FGM-3 has greater values of radial displacement comparing rest materials for k = -2, -1,0,1,2. On the other hand, FGM-1 has lower values for k = 2 in comparison to other materials. Further, FGM-1 shows most compressive displacements among other assumed FGM and non-FGM materials for all considered k. Figure 22, Figure 23, Figure 24 and Figure 25 represent radial stress for different material combinations for considered thickness indices. From these figures, it is marked that FGM-1,2,3 and non-FGM have the lowest and highest magnitude of radial stress at k = 2 and k = -2, respectively as radius tailors from inner to outer. But among all selected materials, FGM-1 has lower and non-FGM has a higher magnitude of radial stress at k = 2.

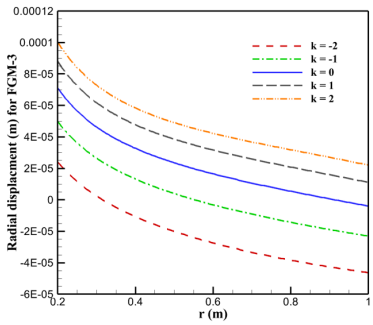

Fig.20 Radial displacement for FGM-3 disk

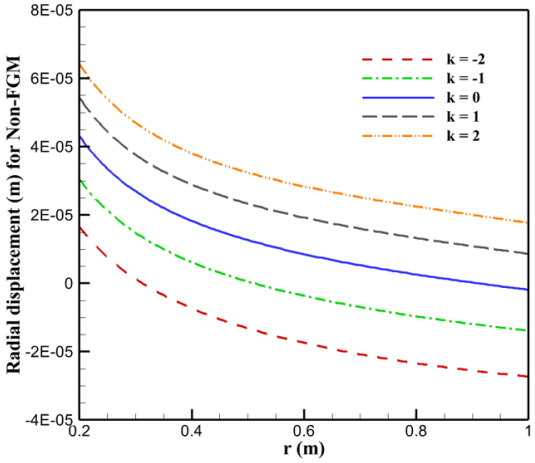

Fig.21 Radial displacement for non-FGM disk

Due to the higher magnitude of radial stress non-FGM is not a preferred material because it does not support the smooth distribution of stress.
As engineers work in the direction of reducing the stress concentration in the mechanical component under the pressure condition so they should use composite material in the place of non-FGM material. Here in this work material comparison is also done that helps in selecting the best materials for the engineering component design.

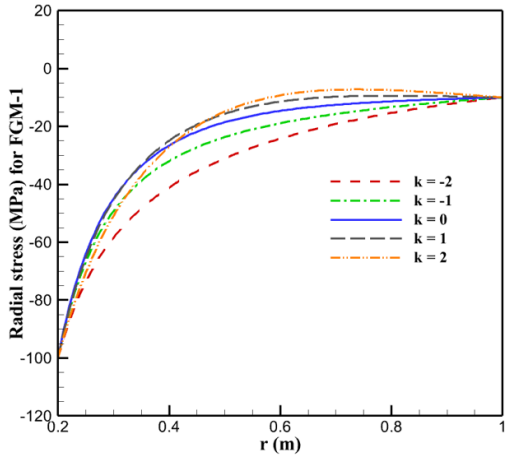

Fig.22 Radial stress for FGM-1 disk

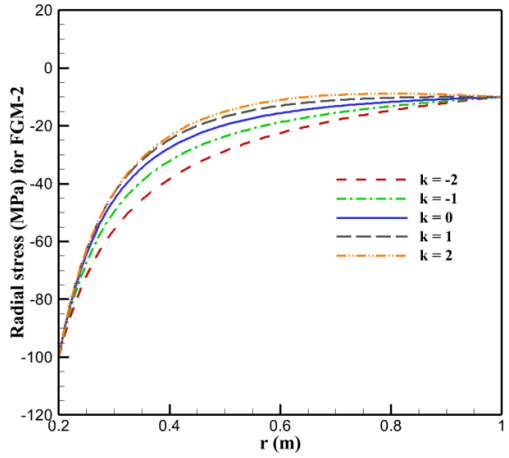

Fig.23 Radial stress for FGM-2 disk

The distribution of tangential stress can be seen for different material combinations in Figure 26, Figure 27, Figure 28 and Figure 29. While looking into these graphs, it is observed that FGM-1, FGM-2, FGM-3, and non-FGM have lower magnitude at k = -2. But on the other hand, FGM-2, FGM-3, and non-FGM have higher magnitude at k = 2. In Figure 26, one can note that FGM-1 achieves a higher magnitude at k = 1 which is also lower in magnitude in comparison to other materials at the same k = 1. It shows that engineers can also use linear thickness to build a mechanical component that can bear high internal and low external pressure as per the requirement.

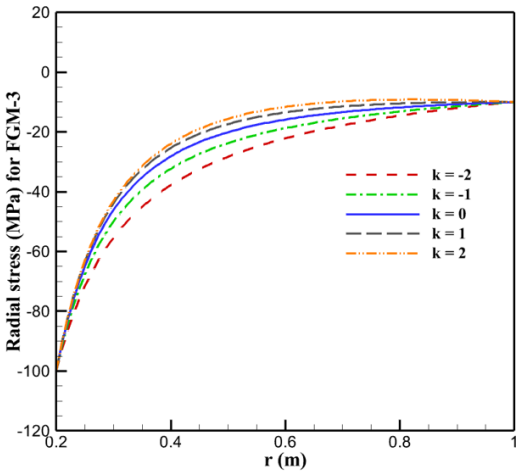

Fig.24 Radial stress for FGM-3 disk

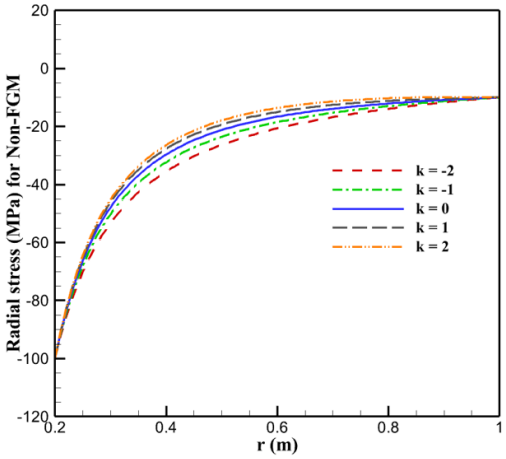

Fig.25 Radial stress for non-FGM disk

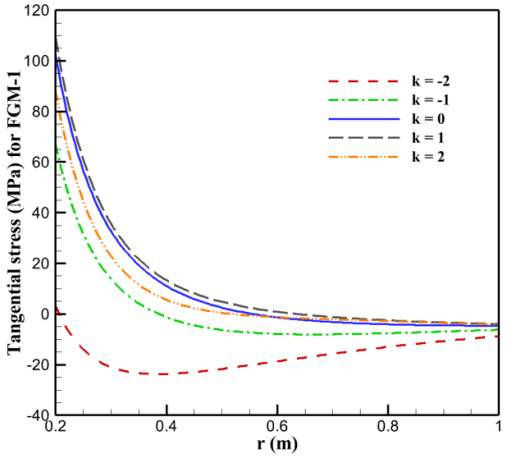

Fig.26 Tangential stress for FGM-1 disk

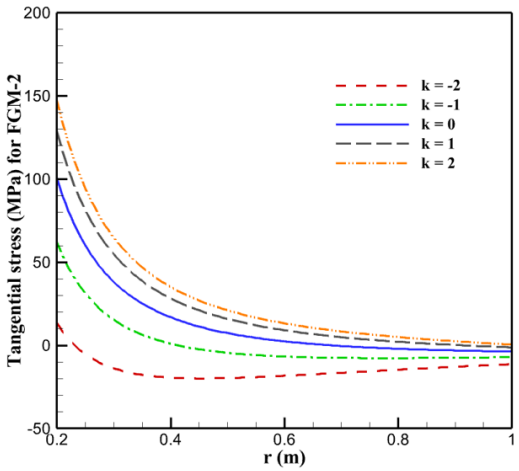

Fig.27 Tangential stress for FGM-2 disk

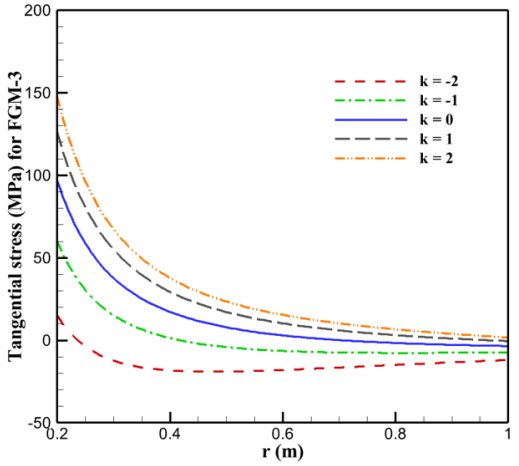

Fig.28 Tangential stress for FGM-3 disk

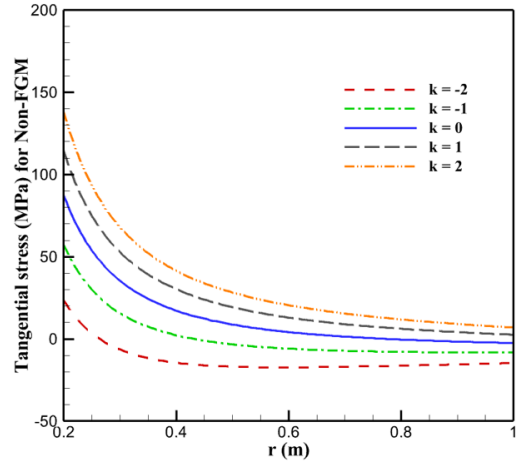

Fig.29 Tangential stress for non-FGM disk

4 Conclusion

In this paper, the applicability of the iterative technique is discussed and a semi-analytical solution for stress and displacement is derived for a thin annular FGM disk under high internal and low external pressure. Young's modulus and thickness of disk are assumed to vary along with exponential law. The three commonly used FGMs are considered for the study. The obtained stress and displacement responses for these three materials are compared with homogenous material. In this study, the following conclusions are made:

- The elastic response of the disk is strongly dependent on the material combination that is chosen as ceramics -metal pairs. Also, the inhomogeneity parameter and thickness of the disk have a great impact on the stress distribution.
- Silicon Carbide - Zinc Alloy (FGM-1) is the best choice among all the considered materials as it comes with a lower magnitude of stress value. This means at the interface of the material; the stress distribution is smoother comparatively in other material combinations.
- The derived results can be used in averting the failure in the design of the annular disk.
- All considered FGMs are better than non-FGM material for the design of annular disks under high internal and low external pressure.
- FGMs used in this study may be helpful to design cutting disk and disk break in vehicles.

Conflict of Interest

There is no conflict of interest was declared by the author.

Appendix

$$A = \left(\frac{(v+2)(m+k)r_1}{3r_2(r_2^2-r_1^2)} + \frac{(v+2)(m+k)}{3r_2(r_1+r_2)}\frac{r_2^2}{r_2^2-r_1^2}\right)$$

$$B = \left(\frac{v(m+k)r_1r_2}{r_2^2-r_1^2} - \left(1+\frac{v(m+k)r_1}{(r_1+r_2)}\right)\frac{r_2^2}{r_2^2-r_1^2}\right)$$

$$C = \left(\frac{q_1}{Y(r_1)} - \frac{q_2}{Y(r_2)}\right)$$

$$D = \left(\frac{q_1r_1^2}{Y(r_1)} - \frac{q_2r_2^2}{Y(r_2)}\right)$$

References:

[1] Nejad, M.Z., Abedi, M., Lotfian, M.H. and Ghannad, M., An exact solution for stresses and displacements of pressurized FGM thick-walled spherical shells with exponential-varying properties, *Journal of mechanical science and technology*, *26*(12), 2012, pp.4081-4087.

[2] Dini, A., Nematollahi, M.A. and Hosseini, M., Analytical solution for magneto-thermo-elastic responses of an annular functionally graded sandwich disk by considering internal heat generation and convective boundary condition, *Journal of Sandwich Structures & Materials*, *23*(2), 2021, pp.542-567.

[3] Jalali, M.H. and Shahriari, B., Elastic stress analysis of rotating functionally graded annular disk of variable thickness using finite difference method, *Mathematical Problems in Engineering*, *2018*.

[4] Temimi, H. and Ansari, A.R., A new iterative technique for solving nonlinear second order multi-point boundary value problems, *Applied Mathematics and Computation*, *218*(4), 2011, pp.1457-1466.

[5] Zamani Nejad, M., Rastgoo, A. and Hadi, A., Effect of exponentially-varying properties on displacements and stresses in pressurized functionally graded thick spherical shells with using iterative technique, *Journal of Solid Mechanics*, *6*(4), 2014, pp.366-377.

[6] Lin, W.F., Elastic analysis for rotating functionally graded annular disk with exponentially-varying profile and properties, *Mathematical Problems in Engineering*, 2020.

[7] Sahni, M. and Mehta, P.D., Thermo-mechanical Analysis of Sandwich Cylinder with Middle FGM and Boundary Composite Layers, *Structural Integrity and Life, 20*(3), 2020, pp.313-318.

[8] Mars, J.A.M.E.L., Koubaa, S.A.N.A., Wali, M.O.N.D.H.E.R. and Dammak, F.A.K.H.R.E.D.D.I.N.E., Numerical analysis of geometrically non-linear behavior of functionally graded shells, *Latin American Journal of Solids and Structures*, *14*, 2017, pp.1952-1978.

[9] Nematollahi, M.A., Dini, A. and Hosseini, M., Thermo-magnetic analysis of thick-walled spherical pressure vessels made of functionally graded materials, *Applied Mathematics and Mechanics*, *40*(6), 2019, pp.751-766.

[10] Çallioğlu, H., Bektaş, N.B. and Sayer, M., Stress analysis of functionally graded rotating discs: analytical and numerical solutions, *Acta Mechanica Sinica*, *27*(6), 2011, pp.950-955.

[11] Kacar, I., Exact elasticity solutions to rotating pressurized axisymmetric vessels made of functionally graded materials (FGM), *Materialwissenschaft und Werkstofftechnik*, *51*(11), 2020, pp.1481-1492.

[12] Bayat, M., Saleem, M., Sahari, B.B., Hamouda, A.M.S. and Mahdi, E., Analysis of functionally graded rotating disks with variable thickness, *Mechanics Research Communications*, *35*(5), 2008, pp.283-309.

[13] Bayat, M., Saleem, M., Sahari, B.B., Hamouda, A.M.S. and Mahdi, E., Mechanical and thermal stresses in a functionally graded rotating disk with variable thickness due to radially symmetry loads, *International Journal of Pressure Vessels and Piping*, *86*(6), 2009, pp.357-372.

[14] Nkene, E.R.A., Ngueyep, L.L.M., Ndop, J., Djiokeng, E.S. and Ndjaka, J.M.B., Displacements, strains, and stresses investigations in an inhomogeneous rotating hollow cylinder made of functionally graded materials under an axisymmetric radial loading, *World Journal of Mechanics*, *8*(03), 2018, p.59.

[15] Delouei, A.A., Emamian, A., Karimnejad, S. and Sajjadi, H., A closed-form solution for axisymmetric conduction in a finite functionally graded cylinder, *International Communications in Heat and Mass Transfer*, *108*, 2019, p.104280.

[16] Nejad, M.Z., Rastgoo, A. and Hadi, A., Exact elasto-plastic analysis of rotating disks made of functionally graded materials, *International Journal of Engineering Science*, *85*, 2014, pp.47-57.

[17] Tutuncu, N., Stresses in thick-walled FGM cylinders with exponentially-varying properties, Engineering *Structures*, *29*(9), 2007, pp.2032-2035.

[18] Zafarmand, H. and Hassani, B., Analysis of two-dimensional functionally graded rotating thick disks with variable thickness, *Acta Mechanica*, *225*(2), 2014, pp.453-464.

[19] Paul, S.K., & Sahni, M., Two-dimensional mechanical stresses for a pressurized cylinder made of functionally graded material, *Structural Integrity and Life - Integritet I Vek Konstrukcija, 19*(2), 2019, 79-85.

[20] Paul, S.K., & Sahni, M., Two- dimensional Stress Analysis of Thick Hollow Functionally Graded Sphere under Non-axisymmetric Mechanical Loading, *International Journal of*

Mathematical, Engineering and Management Sciences, 6(4), 2021, 1115-1126.

[21] Paul, S.K. and Sahni, M., Two-dimensional stress analysis of a thick hollow cylinder made of functionally graded material subjected to non-axisymmetric loading. *Structural Integrity and Life - Integritet I Vek Konstrukcija,* Vol. 21, Special Issue, 2021, pp. S75–S81.

[22] Cem, B.O.Ğ.A., Effect of Inhomogeneity Constant on Equivalent Stresses in Elastic Analysis of Hollow Cylinder Made from Functionally Graded Material, *Gazi University Journal of Science*, *33*(1), 2020, pp.201-212.

[23] Kacar, I., Exact elasticity solutions to rotating pressurized axisymmetric vessels made of functionally graded materials (FGM). *Materialwissenschaft und Werkstofftechnik*, *51*(11), 2020, pp.1481-1492.

[24] Sharma, S. and Sahni, M., Creep Analysis of Thin Rotating Disc under Plane Stress with no Edge load, *WSEAS transactions on applied and theoretical mechanics*, *3*(7), 2008.

[25] Sahni, M. and Sharma, S., Elastic-plastic deformation of a thin rotating solid disk of exponentially varying density. *Research on Engineering Structures and Materials*, *3*(2), 2017, pp.123-133.

[26] Sharma, S., Sahni, M. and Kumar, R., Elastic-plastic analysis of a thin rotating disk of exponentially variable thickness with inclusion, *WSEAS Transactions on Mathematics*, *9*(5), 2010, pp.314-323.

Contribution of individual authors

Sandeep Kumar Paul developed the model and started working on it and obtained the solution by applying iterative technique.
Manoj Sahni examined the theory of validation.
The manuscript was written through the contribution of both authors. Both have discussed the results, reviewed, and approved the final version of the manuscript.

Sources of Funding for Research Presented in a Scientific Article or Scientific Article Itself

This research work is not supported by any funding from public, commercial or not-for-profit sector.

Creative Commons Attribution License 4.0 (Attribution 4.0 International, CC BY 4.0)